

This is the accepted manuscript version of the contribution published as:

Schwenk, C., Freundt, F., Aeschbach, W., **Bohrer, B.** (2022):
Extending noble gas solubilities in water to higher temperatures for environmental application
J. Chem. Eng. Data **67** (5), 1164 – 1173

The publisher's version is available at:

<http://dx.doi.org/10.1021/acs.jced.2c00009>

Extending Noble Gas Solubilities in Water to higher Temperatures for Environmental Application

Cornelis Schwenk,^{†,‡,¶} Florian Freundt,[‡] Werner Aeschbach,[‡] and Bertram
Boehrer^{*,†}

[†]*Helmholtz Centre for Environmental Research - UFZ, 39114 Magdeburg, Germany*

[‡]*Institute of Environmental Physics, Heidelberg University, 69120 Heidelberg, Germany*

[¶]*Now at Johannes Gutenberg University of Mainz, 55128 Mainz, Germany*

E-mail: bertram.boehrer@ufz.de

Phone: +49 391 - 810 9441

Abstract

Noble gas concentrations in natural waters are widely used to determine ambient temperature conditions during the last intensive contact with the atmosphere (equilibration). Such applications require accurate solubility functions, which so far are available only for the common environmental temperature range between (0 and 35) °C. Nonetheless, environmental scenarios that generate higher surface-water temperatures (such as volcanism) exist. Previous solubility measurements beyond ~ 35 °C are sparse or outdated and were determined through equilibration of water with pure noble gases. This can potentially render them not suitable for environmental applications where equilibration with atmospheric air is considered. We therefore conducted new measurements for the solubilities of helium, neon, argon, krypton and xenon in de-ionized water equilibrated with atmospheric air at ~ 1 bar for temperatures ranging from (25

to 80) °C. These measurements were combined with data from literature that was obtained in a similar fashion and fitted with a commonly used function to determine new noble gas solubility functions valid from (0 to 80) °C. We estimate relative standard uncertainties with a 0.99 level of confidence between 0.015 and 0.030 for the new functions which are thus suitable for the investigation of environmental high-temperature equilibration scenarios. For temperatures beyond 35 °C, the new functions deviate significantly from previous studies.

Introduction

Dissolved gases in natural waters are mainly inherited from the atmosphere by equilibrium dissolution and are therefore sensitive to the various conditions of air-water gas exchange. Due to their chemical and biological inertness and their extremely homogeneous distribution in Earth's atmosphere, the noble gases in particular present themselves as ideal geochemical tracers and measurements of their concentrations have widely been used to reconstruct ambient temperatures during the last intensive contact with the atmosphere (equilibration)¹⁻³. This approach is called *noble gas thermometry* and has been applied to track groundwater recharge temperatures⁴⁻⁶, to analyze temperature variations in the past^{1,7,8} and to reconstruct deep ocean recharge temperatures⁹. The main focus of noble gas thermometry has thus been on environmental conditions commonly found in nature, which is why up to date solubility functions do not exceed $\sim 35\text{ °C}$ ¹⁰. However, environmental scenarios that can generate much higher surface-water temperatures exist (volcanic activity etc.), and explicitly allowing for this possibility might help explain noble gas concentration measurements in investigations of such environments.

Previous studies that measured noble gas solubilities beyond $\sim 35\text{ °C}$ are quite old, deliver only sparse data from equilibration with pure noble gases and often conducted experiments under industrial conditions (ultra-high pressures and temperatures, distilled water

completely degassed before equilibration) rather than environmental conditions (pressures of ~ 1 bar, temperatures below 100°C and water that has not been degassed beforehand)^{11–22}. According to Jenkins et al. (2019)¹⁰, using solubility measurements obtained through equilibration with atmospheric air is more wise for environmental purposes than using measurements obtained through equilibration with pure noble gases, since in the latter case i) partial pressures must be extrapolated over many orders of magnitude and ii) the absence of other gases can give rise to co-solvency-induced biases¹⁰. Their example states that when measuring the solubility of 1 bar of Xe one effectively replaces 0.8 bar of nitrogen and 0.2 bar of oxygen with a much more soluble gas that must no longer compete for solution sites. Additionally, a useful advantage of equilibrating water with atmospheric air instead of pure noble gas is that both the true equilibrated concentrations in samples and the calibration of measurements are directly linked to atmospheric air, thereby canceling substantial uncertainties in the absolute mixing ratio of noble gases (in particular the rare Kr and Xe) in air¹⁰. Previous noble gas solubility measurements for temperatures beyond $\sim 35^\circ\text{C}$ are therefore neither reliable nor appropriate for conducting high-temperature noble gas thermometry.

This work aims at removing this shortcoming. We measured noble gas solubilities over the range from (25 to 80°C) by equilibrating de-ionized water with atmospheric air at atmospheric pressures. We combine our data with published solubility data at lower temperatures (Jenkins et al. (2019)¹⁰) to produce new continuous solubility functions over the range from (0 to 80°C) at high accuracy for the implementation of noble gas thermometry at elevated temperatures as they can be expected in volcanic regions of our planet.

Definitions and Units

The water-side concentration $C_{W,i}$ of a noble gas i is related to its solubility L_i and the partial pressure p_i that the gas i exerts on the water surface by

$$C_{W,i} = L_i \cdot p_i. \quad (1)$$

Equation 1 is a form of Henry's law, although it is often written in an inverted form, where the Henry constant is defined as the inverse of the solubility L_i used here. The solubility is solely a function of temperature T . The partial pressure is a function of total atmospheric pressure p_{atm} , the temperature T (since the water vapor pressure e in the surface boundary layer is assumed to be at saturation $e_s(T)$), and the atmospheric mole fraction x_i of the noble gas i . Equation 1 can therefore be written explicitly as

$$C_{W,i}(T) = L_i(T) \cdot (p_{\text{atm}} - e_s(T)) \cdot x_i. \quad (2)$$

In this work the water-side concentrations are given in units of $[C_W] = \text{mol kg}^{-1}$ and the pressures in $[p] = \text{bar}$, giving the solubilities the units $[L] = \text{mol kg}^{-1} \text{bar}^{-1}$. They can however be presented in a multitude of units such as $\text{mol l}^{-1} \text{bar}^{-1}$ or $\text{mol mol}^{-1} \text{bar}^{-1}$ or $\text{cm}^3 \text{STP g}^{-1} \text{atm}^{-1}$ etc., or as pure (unitless) numbers (Bunsen coefficients or Ostwald coefficients) by relating concentrations of dissolved noble gases (at given temperature) to concentrations in the air space²³. See the supplementary material for some examples of solubility unit conversions.

Methods

Measurements of noble gas solubilities were conducted with atmospheric air instead of pure noble gases as this circumvents potential problems that result from the extrapolation of partial pressures over many orders of magnitude and the emergence of co-solvency-induced

biases¹⁰. The equilibration procedure was inspired by Jenkins et al. (2019)¹⁰, who measured the noble gas solubilities in water from (0 to 35) °C through equilibration with marine atmospheric air, since we ultimately combined our noble gas solubility measurements with synthetic data produced from the Jenkins solubility functions.

Equilibration

Whereas Jenkins et al. (2019)¹⁰ equilibrated de-ionized water with ocean air taken from the sea side, we 'used' the outside air in Magdeburg, Germany, by opening the windows and letting the water equilibrate with the laboratory air, which was sampled at two different times during our experimental phase (the equilibration setup is depicted in Figure 1). De-ionized water was filled into a *Julabo SP-450* Refrigerated-Heating Circulator (capable of thermal regulation to ± 0.01 °C) and heated to a constant temperature. The air and water temperatures were recorded using two Fluke temperature probes connected to a Fluke 1529 Chub-E4 Thermometer (accuracy of at least ± 0.01 °C) and logged by a computer in five second intervals. An internal *Julabo* pump (0.5 bar, 22 l/min) and an additional *Elegant Comet* water pump (0.5 bar, 12 V, 10 l/min) installed in the bath ensured thorough mixing of the entire water volume and significant water-surface roughness without bubble formation or overly chaotic surface behavior. Due to evaporation, the volume of water (ca. 20 L) was not constant during equilibration but varied by no more than 2 L. In order to enforce 100% vapor saturation in the gas-water boundary layer as well as possible, a hood of styrodur was built to fit neatly onto the temperature bath. The hood was not gas-tight and allowed for some in- and outflow of air (and thereby did not allow for a pressure difference between the in- and outside), but suppressed turbulence and dry-air inflow. The hood could be taken on and off, but was always kept on during equilibration. Contents within the hood are referred to as the *equilibration chamber*. For experiments at high temperatures a large plastic bag was sometimes fixed onto the hood so that the air flux, and thereby the inflow of dry air that could "erode" the gas-water boundary layer, was reduced. The initial plan

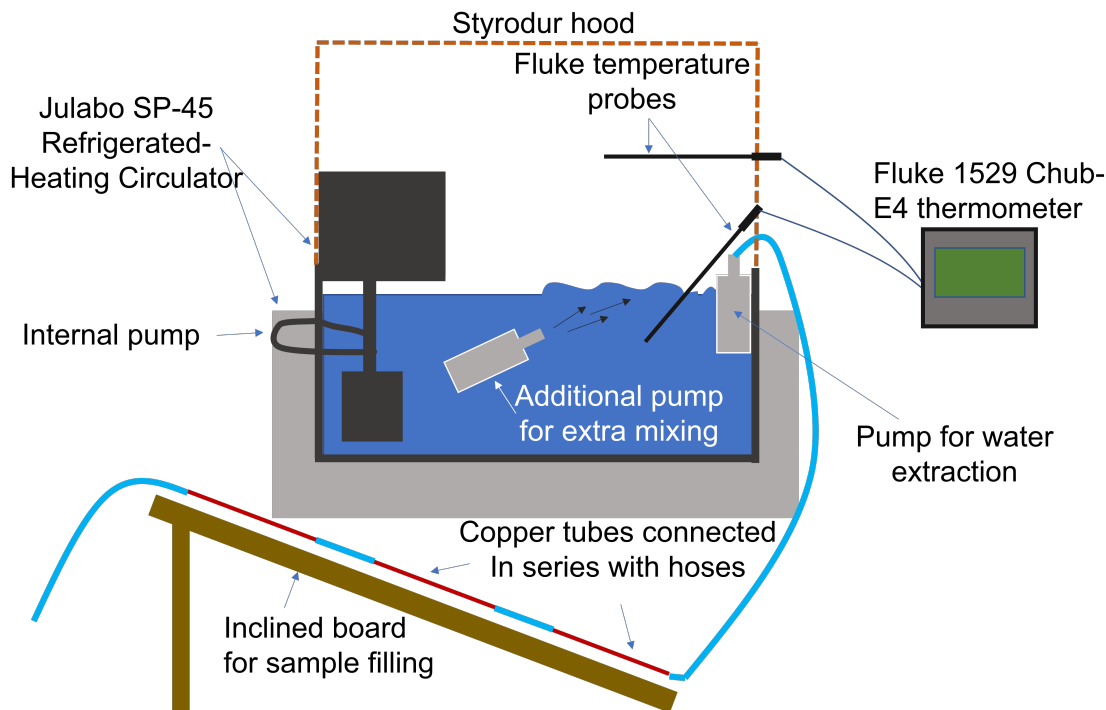


Figure 1: Experimental setup of the equilibration procedure. A *Julabo SP-450* Refrigerated-Heating Circulator was capped off with a styrodur hood, an internally and an externally installed pump thoroughly mixed the water, Fluke probes measured the water and air temperature throughout the equilibration and copper tubes connected in series to a pump were used for sampling.

was to leave the windows open during equilibration to ensure constant atmospheric noble gas composition, but since our experiments were undertaken in the winter, in-flowing cold (and dry) outside air increased the temperature difference between the gas volume and water inside the equilibration chamber significantly. This was sure to reduce the vapor content and endanger the assumption of 100% vapor saturation in the boundary layer, thus leading to unpredictable gas-exchange behavior introducing possibly large, unquantifiable uncertainties. To avoid this the windows were kept closed for the equilibration period and it was assumed that the gas volume of the laboratory was large enough to present the ca. 20 L of water with an effectively infinite reservoir of atmospheric gas. Throughout the experimental phase ventilation in the lab was turned permanently off, such that neighboring labs wouldn't contaminate our laboratory air with extra or non-atmospheric gasses. Air pressure was measured at the beginning and end of equilibration using a *Kestrel 5700* hygrometer. To

determine air pressure variation during the equilibration period, hourly pressure data from the weather station 03126 in Magdeburg, operated by the German Weather Service (DWD), was used (source: Deutscher Wetterdienst). Before each equilibration the hood was removed and the windows opened for a long period of time such that the laboratory air was renewed and the gas composition could become adequately atmospheric.

Sampling

Another *Elegant Comet* water pump installed within the water bath and was used after equilibration to pump the water out of the bath through an initially empty (air-filled) translucent plastic hose into three copper tubes that were installed in series (connected by short plastic hoses) on an inclined board. Pressure induced at the inlet as opposed to the outlet avoided potential degassing during sampling. The highly pure copper is sturdy, extremely tight regarding leakage and can allow year-long storage of water samples without loss of noble gases¹. Similarly to field sampling, plenty of water from the temperature bath was flushed through the samplers while the rails were struck using a wrench such that any gas bubbles stuck on the insides would release. This was done until we were confident that there were few if any gas bubbles remaining. The copper tubes were then manually sealed using a wrench and the pump consequently turned off.

Equilibration Time Scales

To guarantee an approximation of gas concentration to equilibrium within better than 1% we needed to quantitatively evaluate the equilibration time scales. Jenkins et al. (2019)¹⁰ argue that the gas transfer time scale (or also *response time*) τ_i for a specific gas i is given by:

$$\tau_i = \tau_0 S c_i^\alpha, \quad (3)$$

where $Sc_i \equiv \frac{\nu}{D_i}$ is the Schmidt number (ratio of the kinematic viscosity ν of water to the diffusivity D_i of the gas i), $\alpha \in R$ is the Schmidt number exponent and τ_0 is a constant dependent on the experimental setup (geometry of the water bath, fluid motion induced by the pumps etc.). The Schmidt number is commonly used to compare momentum and gas transport in water and is dependent on water temperature and gas-species^{24,25}. The Schmidt exponent α can vary from 1/2 to 1, depending on the gas exchange model and the surface roughness; for a smooth surface the exponent should be close to 2/3, for a rough surface closer to 1/2²⁴. We chose to set the equilibration time scale τ_{eq} as the time it takes for the concentration to approach $C(t = \infty) =: C_\infty$ by a factor of $1/e$. Assuming an exponential approximation of the equilibrium delivers:

$$C(t) = (C_0 - C_\infty) \cdot \exp(-t/\tau_{\text{eq}}) + C_\infty. \quad (4)$$

Hence, in the extreme case of an initial concentration of zero, equilibration must run for $t = 5\tau_{\text{eq}}$ to reach a concentration within 1% of C_∞ , ($e^{-5} \cdot 100\% = 0.67\%$). To determine the response time, oxygen was selected as a gas that can be easily surveyed with sensors. Initial experiments were conducted where water in the bath was rapidly heated (or cooled) from one temperature T_1 to another T_2 , thereby inducing an oxygen over-saturation (or under-saturation). The oxygen content was then measured in real time and τ_{eq} determined by fitting the natural logarithm on our continuous oxygen saturation measurements $\xi(t)$ minus the equilibrium saturation ξ_∞ with a linear function:

$$\ln(\xi(t) - \xi_\infty) = a \cdot t + b, \quad (5)$$

with the response time resulting from

$$\tau_{\text{eq}} = a^{-1}. \quad (6)$$

If the equilibration time scales $\tau_{\text{eq},1}$ and $\tau_{\text{eq},2}$ are measured in this way for one gas at two different temperatures T_1 and T_2 , with the Schmidt numbers Sc_1 and Sc_2 known for both temperatures, one can determine α using:

$$\alpha = \frac{\ln\left(\frac{\tau_{\text{eq},1}}{\tau_{\text{eq},2}}\right)}{\ln\left(\frac{Sc_1}{Sc_2}\right)}. \quad (7)$$

According to equation 3, the constant τ_0 can then be determined by arithmetically averaging different equilibration experiments:

$$\tau_0 = \frac{1}{n} \cdot \sum_{j=1}^n \tau_{\text{eq},j} Sc_j^{-\alpha}, \quad (8)$$

for $j \in \{1, 2, \dots, n\}$, the experiment undertaken at temperature T_j . It is therefore possible to determine the equilibration time scale of the experiment for one gas by measuring the equilibration behavior of another, as long as the Schmidt numbers are known for both and one assumes that in equation 3, α and τ_0 are independent of the gas in question. Heavier noble gases have higher Schmidt numbers than lighter ones²⁵ and the Schmidt number reduces with increasing temperature. From equation 3 it is clear that higher Schmidt numbers cause longer equilibration times. One will therefore find the longest equilibration time scale for xenon at the coldest water temperature at which an equilibration is conducted (25 °C). We determined a value of $\alpha \approx 0.6$, which corresponds to a smooth water surface, and a value of $\tau_0 = 1.3$ min. This gives us an equilibration time scale τ_{eq} of:

$$\tau_{\text{eq}} = 1.3 \cdot Sc^{0.6} \text{ min}. \quad (9)$$

By inserting the Schmidt number for xenon at 25 °C of 609 (taken from Jähne et al. (1987)²⁵) into Equation 9, a maximum equilibration time of $\tau_{\text{eq}} \approx 60$ min was determined. Each experiment was thus run for at least five equilibration time scales (> 5 h) and often longer, i.e. overnight, such that a final concentration within $e^{-5} \cdot 100\% < 1\%$ of the true equilibrium

concentration C_∞ was achieved.

Moist Boundary Layer Considerations

Calculating the noble gas solubility $L_i(T)$ from measurements of the concentration $C_i(T)$ (Equation 2) requires that the total pressure exerted by the dry atmosphere $p_{\text{atm}}(z) =: p_{\text{tot}}$ be corrected to account for the saturation vapor pressure $e_s(T)$. The assumption underlying this equation is that the air-water boundary layer controlling equilibration is at 100% saturation with respect to the water temperature, even if the air above is dry (Figure 2). Turbulence in the free atmosphere reduces as the water surface is approached. A layer of ~ 1 mm thickness called the *molecular-viscous layer* above the surface experiences no turbulence and all transport is purely governed by molecular diffusion²⁴. Here the boundary layer vapor pressure $p_{\text{vap}}^{\text{BL}}$ is assumed to equal the saturation vapor pressure corresponding to the water surface temperature $e_s(T_{\text{water}})$. During our experiments we observed that once 50°C were

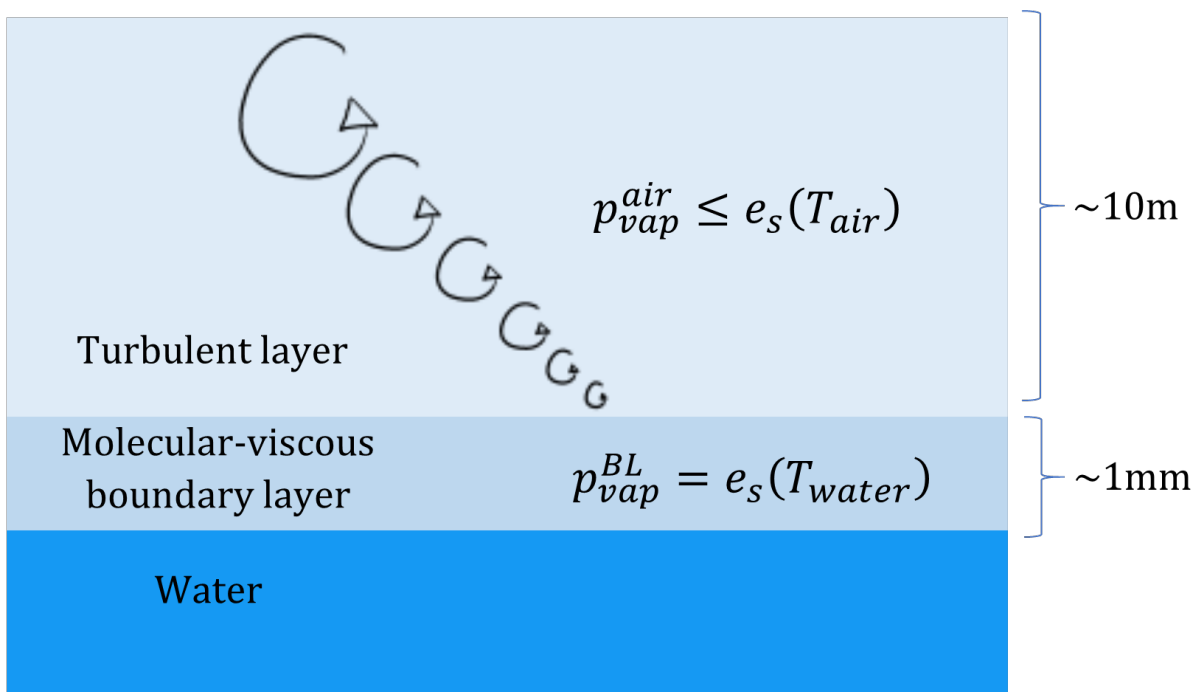


Figure 2: Schematic of the boundary layer conditions assumed upon equilibration. The vapor pressure p_{vap} in the molecular-viscous boundary layer is assumed to be equal to the saturation vapor $e_s(T_{\text{water}})$, even if the air above is relatively dry.

exceeded, the temperature difference between the water and air in the equilibration chamber ΔT became significant ($\Delta T \approx 12^\circ\text{C}$), even when multiple attempts were made to thermally insulate the setup while allowing for gas exchange to avoid pressure differences between the in- and outside. We decided to investigate whether this temperature difference could affect oxygen saturation by changing ΔT abruptly. The effect of air temperature on the oxygen saturation turned out to be so small that it fell below the detection limit of 1%. This provides strong evidence that the air and water surfaces come into thermal equilibrium at the water temperature even if the equilibration chamber temperature is a few degrees cooler.

Calculating Saturation Vapor Pressure

Calculating the solubility from a concentration measurement using Equation 2 requires the saturation vapor pressure $e_s(T)$. The *Magnus formula* is most commonly used²⁶. It stems from the simple integration of the Clausius-Clapeyron relation under assumption of a constant latent heat. Alduchov and Eskridge (1996)²⁶ improved this approach and their equation recommended from (-40 to 50) $^\circ\text{C}$ ²⁶. For higher temperatures the IAPWS adopted the function

$$\ln \left(\frac{e_s(T)}{e_{s,c}} \right) = \frac{T_c}{T} [a_1\tau + a_2\tau^{1.5} + a_3\tau^3 + a_4\tau^{3.5} + a_5\tau^4 + a_6\tau^{7.5}], \quad (10)$$

developed by Wagner and Pruss (1993)²⁷, where T_c is the critical temperature of water, T is in Kelvin, $e_{s,c}$ is the critical vapor pressure, $\tau = 1 - \frac{T}{T_c}$ and $e_s(T)$ has the unit MPa ²⁸. The conversion to bar is trivial. The coefficients can be found in the cited publication. This function was used in this work since it is very accurate and valid up to 374°C .

Mass Spectrometric Measurements

The *GV Instruments MM5400* mass spectrometer of the Institute for Environmental Physics, Heidelberg (IUP) was utilized to determine the noble gas concentrations of samples. Measurements are conducted in three stages: gas preparation, mass spectrometer measurements

and subsequent data evaluation. The general procedures as well as the system performance are similar to the methods presented by Beyerle et al. (2000)²⁹.

Gas Preparation

Water samples contained within copper tubes are extracted into an inlet volume evacuated to pressures no larger than 10^{-2} mbar. Dissolved noble gases then diffuse into the gas phase due to the lower partial pressure. With the help of a magnetic stirrer the roughly 20 ml of water are completely degassed over a period of 50 minutes, providing an extraction effectiveness of 99.99% for all noble gas species³⁰. Gas flow is ensured by drying the gas at room temperature in a trap whose volume is composed of zeolith granules with a pore size of 3Å. Saturation of the trap after 4-5 water sample measurements necessitates heating to 230 °C for 3-4 hours to dry it of adsorbed H₂O³⁰. In the next step, one can separate and purify the gases by exploiting differences in adsorption temperatures by means of a cryostatic cooling system. Argon, krypton and xenon adsorb in a stainless steel trap (SST) at 35 K, 45 K and 70 K and desorb at 50 K, 85 K and 110 K, respectively³⁰. These three gases are therefore frozen onto a SST at 25 K; helium and neon are frozen onto an activated charcoal trap (ACT) at 10 K³¹. The individual gas species can thereafter be separated by heating/cooling either trap to the respective adsorption/desorption temperatures. Purification from other gases such as nitrogen, oxygen and hydrogen is accomplished by a series of getter pumps.

Helium is the first gas to be released from the ACT at 42 K. Due to a large range of naturally occurring helium concentrations it is necessary to check the gas amount in a quadrupole mass spectrometer and circumstantially dilute (split) the helium volume until a level is reached that does not saturate the MM5400 spectrometer detectors. Neon undergoes the same procedure after being released from the ACT at 140 K^{30,31}. Krypton and later xenon are then desorbed from the SST, cleansed of argon, and measured. Due to its high concentration argon does not need to be separated from the far less abundant krypton and xenon components

but it too needs to be split before entering the spectrometer. Getter pumps situated before and within the MM5400 ensure that some of the remaining gases such as H_2 are removed³¹. Once the last noble gas measurement is underway the SST and ACT can be heated to room temperature and pumps can cleanse them of remaining gases.

Mass Spectrometer Measurements

The mass spectrometer consists of an ion source, a magnet and two detectors. Moving ionized atoms are deflected in a magnetic field by the Lorentz force at a typical radius of curvature dependent on the mass to charge ratio. The mass spectrometer can therefore discriminate mass-to-charge ratios. Naturally abundant noble gas isotopes (^4He , ^{20}Ne , ^{22}Ne , ^{36}Ar , ^{40}Ar) are detected by a Faraday cup, and naturally less abundant noble gas isotopes (^3He , ^{84}Kr , ^{132}Xe) by an electron multiplier.

Ultimately the spectrometer measures count rates (and therefore peak heights) of ionic impacts. To measure noble gas amounts one must therefore routinely implement calibration measurements of the entire device using gaseous samples of known composition³⁰. In these calibrations (called Cals), atmospheric air of known volume (and noble gas composition) is sent through the entire gas preparation process and respective peak heights are measured. The noble gas amount contained within a sample can thereafter be determined by comparing the measured peak heights to those measured during calibration measurements. The implementation of Cals is crucial since the entire process of noble gas preparation, ionization and detection is strongly non linear with respect to gas amounts³⁰. Cals with different known gas amounts can be realized by admitting varying numbers of exactly calibrated air aliquots to the preparation and measurement process. To compensate for short-term fluctuations in detector sensitivity, fast calibrations (FastCals) are performed. In this case, pure noble gases (He, Ne, Ar+Kr+Xe) are directly led into the spectrometer. This is done imminently before each single measurement.

Mass Spectrometer Data Evaluation and Quality Control

The mass spectrometer data is evaluated using a customized software that calculates noble gas amounts by comparing measured peak heights of a sample with a fit function through the calibration measurements in dependence of their size. Gas amounts are given in cm^3STP (cubic centimeters at standard temperature and pressure $T_0 = 273.15\text{ K}$, $P_0 = 1013.25\text{ mbar}$). The evaluation software allows for sensitivity adjustments, deletion of outliers and corrections for detector non-linearity, among other things. Uncertainties of the calculated calibrated gas amounts are estimated from the reproducibility of the Cal measurements relative to their fit function. The copper tubes containing the water samples are weighed to high precision (0.01 g) before and after the measurement procedure, thus delivering the mass of water contained within. Dividing the gas amounts obtained from the evaluation software by this mass then finally gives noble gas concentrations in $\text{cm}^3\text{STPg}^{-1}$. This is converted to $\text{mol kg}^{-1}\text{ bar}^{-1}$; the explicit procedure can be found in the supplementary material. All measurements are listed in Table 1.

The performance of the analytical system has been thoroughly tested³². The reproducibility of the gas preparation and mass spectrometric analysis follows directly from the repeated calibration measurements and yields typical relative analytical standard uncertainties (compare Table 1) well below 0.01 for noble gases measured on the Faraday detector (He, Ne, Ar) and between 0.01 and 0.02 for the gases analysed with the less stable electron multiplier (Kr, Xe). Repeated analyses of water standards taken from a lake show that these reproducibilities are accurate estimators for the precision of concentration measurements on environmental water samples, even over the time scale of several years including several different measurement runs³². Determination of the absolute accuracy can be done by the analysis of equilibrated water and reference to published solubilities²⁹ or by the analysis of air samples to test the gas sample inlet system³². We regularly conduct such exercises and take measures to correct possible biases³². In regular measurement runs we have no indi-

cations of systematic biases that are significant compared to the statistical errors discussed above. Finally, it should be noted that possible systematic errors related to the uncertainty of the air standard composition cancel in our method of determination of solubilities using air-equilibrated samples¹⁰.

Fitting Noble Gas Solubilities

Solubilities $L_i(T)$ were calculated from measured concentrations $C_i^{\text{meas}}(T)$ for the equilibration temperature T according to Equation 2:

$$L_i(T) = \frac{C_i^{\text{meas}}(T)}{(p_{\text{atm}} - e_s(T)) \cdot x_i}, \quad (11)$$

where p_{atm} is the pressure measured during equilibration and x_i is the atmospheric abundance of the noble gas i , for which we take the generally accepted values that were also used by Jenkins et al. (2019)¹⁰ and listed in Table 2. The standard uncertainty $u(L_i(T))$ is determined through Gaussian error propagation using the concentration measurement standard uncertainty $u(C_i^{\text{meas}}(T))$:

$$u(L_i(T)) = \frac{u(C_i^{\text{meas}}(T))}{(p_{\text{atm}} - e_s(T)) \cdot x_i}. \quad (12)$$

All other quantities can be measured much more accurately. The solubility $L_i(T)$ can be translated into the moist equilibrium concentration $C_i^*(T)$ in mol kg^{-1} as determined by Jenkins et al. (2019)¹⁰ through:

$$C_i^*(T) = L_i(T) \cdot (1.01325\text{bar} - e_s(T)) \cdot x_i. \quad (13)$$

Table 1: All concentration measurements and their standard uncertainties u (0.68 level of confidence) utilized in the fitting procedure, given in mol kg^{-1} .

Exp	He (10^{-8})	$u(\text{He})$ (10^{-10})	Ne (10^{-7})	$u(\text{Ne})$ (10^{-10})	Ar (10^{-4})	$u(\text{Ar})$ (10^{-6})	Kr (10^{-8})	$u(\text{Kr})$ (10^{-10})	Xe (10^{-9})	$u(\text{Xe})$ (10^{-11})
25(i)	0.198	0.111	0.08	0.308	0.126	0.056			0.378	0.583
35(i)	0.194	0.108	0.075	0.29	0.106	0.048	0.218	0.433	0.286	0.458
39(i)	0.192	0.108	0.073	0.282	0.099	0.045	0.197	0.357	0.257	0.436
44(i)	0.189	0.106					0.18	0.346	0.23	0.371
49(i)					0.086	0.037	0.166	0.338	0.208	0.414
50(i)							0.16	0.318		
55(i)	0.187	0.104	0.068	0.264	0.078	0.035			0.186	0.364
60(i)	0.176	0.099	0.062	0.242	0.071	0.032	0.13	0.269	0.163	0.267
65(i)	0.171	0.096	0.06	0.233	0.065	0.029	0.117	0.235	0.145	0.292
70(i)	0.162	0.091	0.055	0.211	0.058	0.026	0.103	0.24		
75(i)	0.15	0.084			0.051	0.023	0.088	0.214	0.109	0.218
80(i)			0.042	0.163			0.073	0.205	0.088	0.191
30(ii)	0.3	0.44			0.125	0.065			0.338	0.529
44(ii)	0.186	0.281			0.089	0.046	0.179	0.326	0.23	0.373
50(ii)	0.246	0.371			0.091	0.047			0.212	0.356
70(ii)					0.058	0.024	0.104	0.219	0.121	0.242
75(ii)							0.089	0.188	0.103	0.217
80(ii)	0.168	0.253			0.046	0.025			0.089	0.169

Table 2: Atmospheric (mole fraction) abundances x_i of noble gases.

Gas	$x_i \times 10^{-6}$
He	5.24
Ne	18.18
Ar	9340
Kr	1.14
Xe	0.087

Synthetic 'data points' at the temperatures measured by Jenkins et al. (2019)¹⁰ were calculated using the Jenkins solubility functions at the temperatures they conducted their experiments at and appended to our measurements. All of these data points were then fitted as one 'data set' using the python package *scipy.optimize.curve_fit*³³. A generalized Valentiner equation^{18,34,35} similar to the one used by Jenkins et al. (2019)¹⁰ was used as the fit function (T in Kelvin):

$$L_i(T) = \exp\left(A + B\frac{100}{T} + C \ln\left(\frac{T}{100}\right) + D\frac{T}{100}\right). \quad (14)$$

The residual of a data point $L_i(T)$ to the fit $L_i^{\text{fit}}(T)$ is calculated by

$$\text{res}_i(T) = \frac{L_i(T) - L_i^{\text{fit}}(T)}{L_i(T)} \times 100\%, \quad (15)$$

and the standard error $u(\text{res}_i(T))$ is calculated through Gaussian error propagation:

$$u(\text{res}_i(T)) = \frac{L_i^{\text{fit}}(T)}{L_i(T)^2} \cdot u(L_i(T)) \times 100\%. \quad (16)$$

We postulated that good measurements must agree with the fit curve within 2%. The worst outliers were removed and the fitting procedure was redone with the remaining data points. This procedure was repeated until all data points agreed with the fit within 2%.

Results and discussion

In total, 13 successful equilibration experiments covering the range of (25 to 80) °C were undertaken. They were named after the approximate temperature they were conducted at ('30' for $T_{\text{water}} \approx 30$ °C). Table 3 lists the experiments and number of analyzed samples under 'Exp' and also the parameters determined from temperature and pressure measurements that are necessary when calculating the solubility. The average water temperature T_{water} and the standard errors $u(T_{\text{water}})$ were determined by averaging the last two hours of temperature measurements and taking the standard deviation. T_{water} is set as the equilibration temperature T for the respective experiment and is used when fitting measurements. The equilibration chamber air temperature T_{air} was determined identically. The final laboratory air pressure p_2 is used when calculating the solubilities. The final pressure standard error $u(p_{\text{DWD}})$ is taken as the standard deviation of the hourly pressure values delivered by the DWD during equilibration. Experiment 65 is presented in detail in the supplementary information as an example.

Table 3: Equilibration experiments with the number of samples analyzed, water temperature T_{water} , air temperature in the equilibration chamber T_{air} , atmospheric pressure p and their variabilities during the experiment.

Exp	$T_{\text{water}}/^\circ\text{C}$	$u(T_{\text{water}})/^\circ\text{C}$	$T_{\text{air}}/^\circ\text{C}$	$u(T_{\text{air}})/^\circ\text{C}$	p/hPa	$u(p_{\text{DWD}})/\text{hPa}$
25 (2)	24.972	0.003	27.02	0.21	1021.1	1.2
30 (2)	30.000	0.004	29.79	0.08	1021.0	0.5
35 (1)	34.964	0.003	36.08	0.16	1018.0	0.5
39 (1)	39.419	0.003	38.26	0.02	1014.0	1.3
44 (2)	43.933	0.003	41.61	0.07	1003.7	0.8
49 (1)	48.948	0.006	39.28	0.50	1022.0	0.5
50 (2)	49.920	0.004	43.64	0.05	998.2	1.7
55 (1)	55.007	0.001	44.32	0.07	1022.0	0.3
60 (1)	60.084	0.001	49.00	0.06	998.7	0.6
65 (1)	65.068	0.001	52.93	0.07	1000.2	0.2
70 (2)	70.055	0.002	58.31	0.79	1000.4	0.1
75 (2)	75.000	0.004	65.66	0.14	1004.5	0.1
80 (2)	80.023	0.002	71.27	0.15	1002.7	0.2

The coefficients obtained for Equation 14 are listed in Table 4. To obtain fit functions that deviate less than 1% from the original curves, the coefficients must not be rounded off to less than three digits after the decimal point (± 0.001). It is however advised to use the coefficients exactly as listed. Figure 3a) presents all data points (synthetic Jenkins data and from this work) incorporated in the final fitting iteration and the resulting solubility functions, and Figure 3b) the residuals to that fit function in percent. Figure 4 shows the histograms of residuals for each noble gas.

Table 4: Coefficients for Equation 14 determined in this work.

	He	Ne	Ar	Kr	Xe
<i>A</i>	-83.6968	-180.5803	-88.6462	-36.0369	-142.0303
<i>B</i>	106.0200	240.6222	122.8871	54.1959	202.7448
<i>C</i>	51.7624	137.8721	48.6396	1.5299	88.9096
<i>D</i>	-5.4664	-19.6012	-4.1208	3.4176	-9.5677

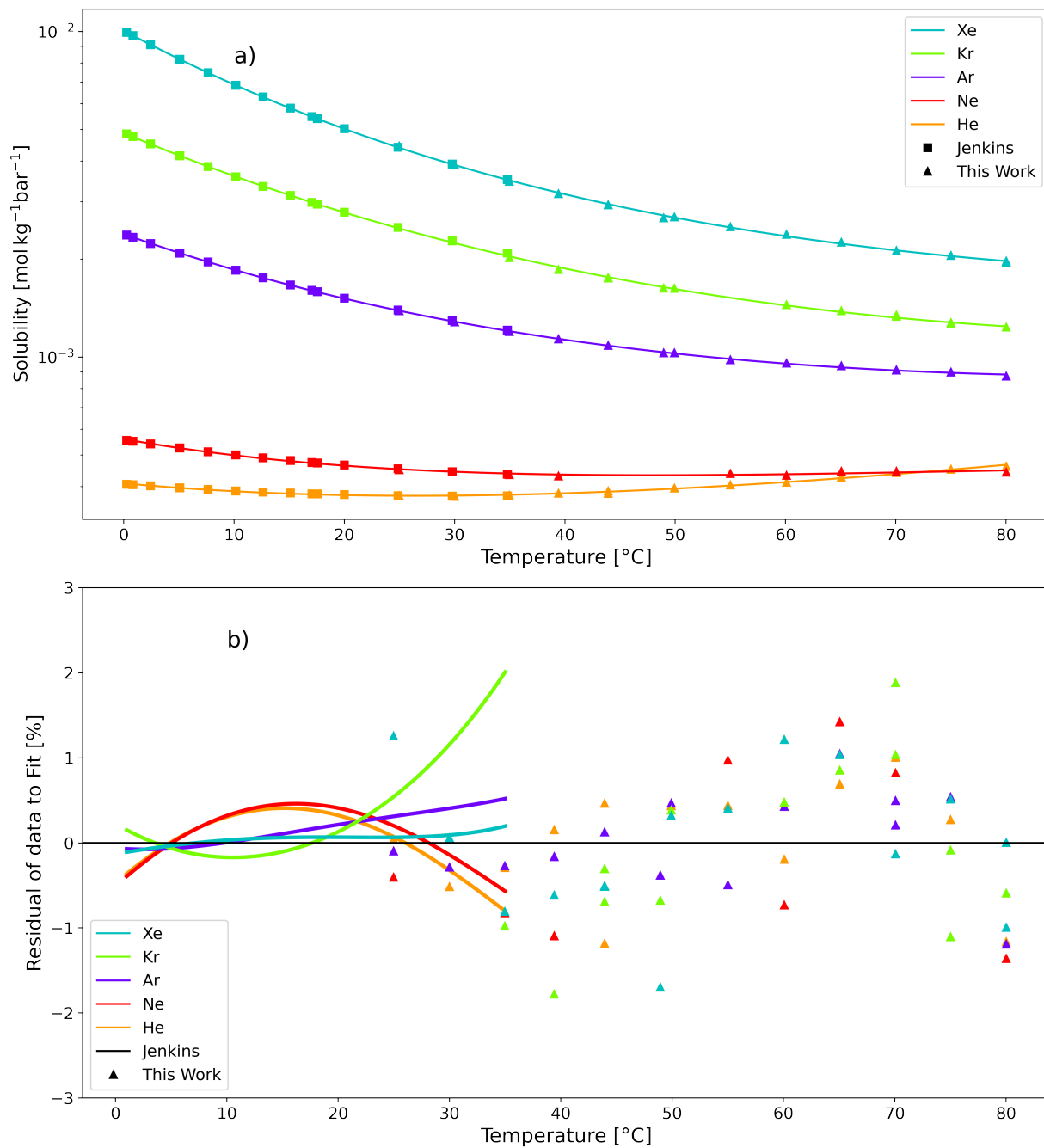


Figure 3: a) Synthetic Jenkins solubilities (solid lines) and solubility data from this work (triangles) for all noble gases fitted (solid line) displayed with a logarithmic y-axis; b) the residuals in percent of that data (triangles) to the fit. The Jenkins solubility functions are plotted as solid lines. Error bars are not plotted for visual clarity but can be seen in the supplementary material.

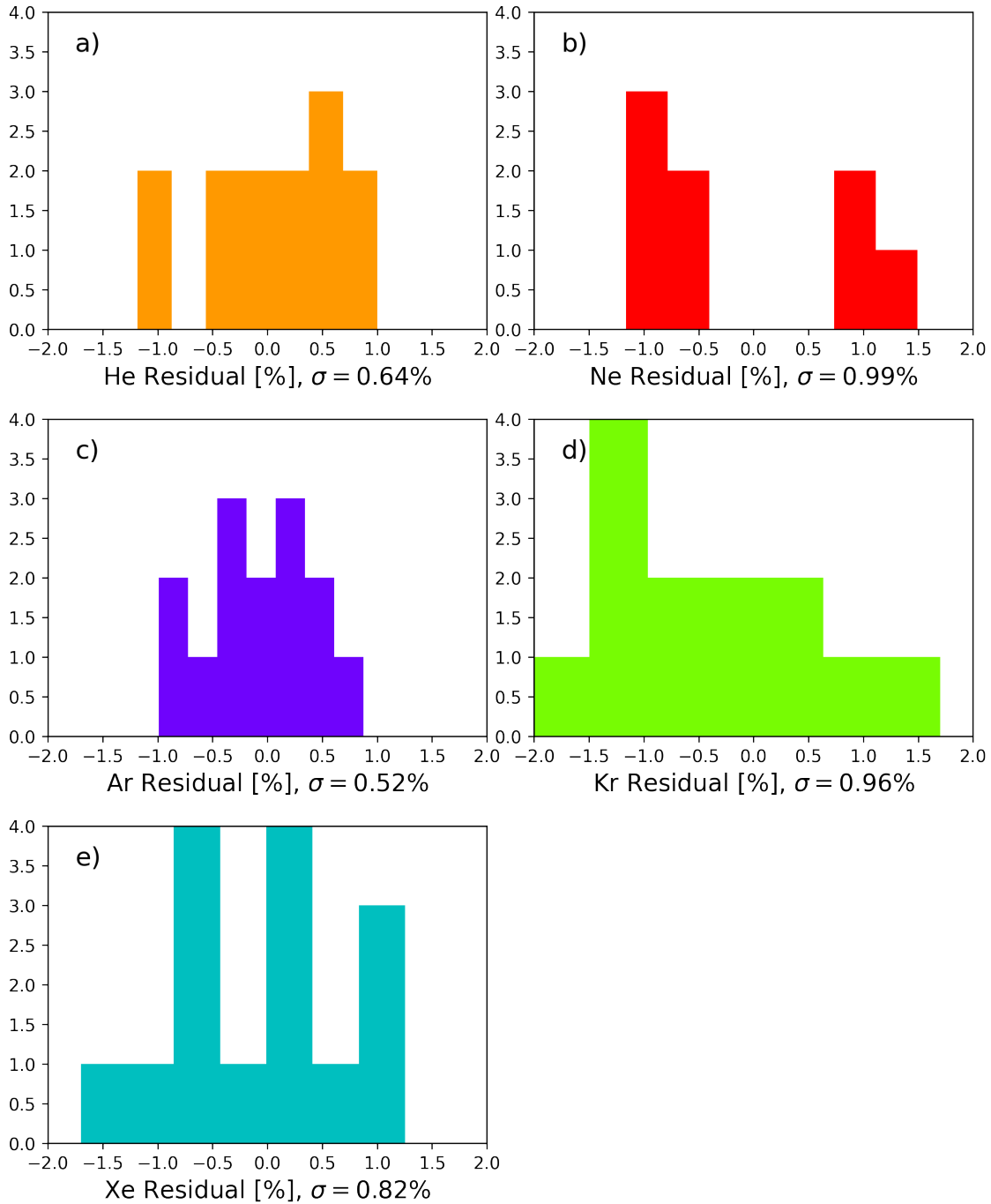


Figure 4: Histograms of residuals to fit for data obtained in this work (i.e synthetic Jenkins data not included) for a) helium, b) neon, c) argon, d) krypton and e) xenon. The standard deviation, labeled on the respective x-axes, is lowest for argon and helium, with almost all points falling within 1.0%. For krypton and neon the standard deviation is largest, with neon suffering from the smallest statistics and krypton showing a systematical deviation to a negative residual. Xenon has a moderate standard deviation and most points lie within a 1.0% residual.

Discussion of New Solubility Functions

Combining our new data with the published data by Jenkins et al. (2019)¹⁰ documents the solubility of the noble gases helium, neon, argon, krypton and xenon over the temperature range (0 to 80) °C (Fig. 3). While in the case of xenon, krypton, and argon solubilities continuously fall over the entire temperature range, solubilities of neon only vary slightly and in the case of helium, even a clear rise of solubility towards higher temperature can be detected, which is an effect of the entropy term in the van't Hoff equation¹. Residuals remain in an acceptable range (mostly around 1% and never more than 2%) for both the Jenkins functions as well as the single experiments from this publications (Fig. 3b). The transition between the two data sets is smooth, only in the case of krypton we see a slight inconsistency between the data sets in the transition of about 3%, which shows that our data lies lower than the fit by Jenkins. This is little more than the estimated accuracy of our measurements permit. Other experiments on solubilities of noble gases (Morrison and Johnstone 1954; cited in Clever 1979a, b, 1980) have been conducted at different conditions hence are not suitable for a crucial comparison at the required accuracy and hence do not help to resolve this issue.

Uncertainties in solubility calculations

Any corrections in solubility calculations that would consider the uncertainties presented in Table 3 would result in relative standard uncertainties $u_r(L)$ no larger than 0.001 and are unnecessary considering the ~ 0.02 relative standard uncertainties of the noble gas measurements.

Comparison with Jenkins solubilities

The Jenkins solubility functions¹⁰ are the most up to date and are based on very high-precision measurements. Figure 5a shows the residuals of the Jenkins solubility functions to the newly determined ones in the range (0 to 35) °C for all noble gases. It is pleasing

to see only small residuals on the order of 0.5% for all gases except krypton, where the residual reaches 2%. This shows that the data from this work is in good agreement with the data from Jenkins, although the krypton data from this work shows a negative systematic deviation compared to the data from Jenkins et al. (2019)¹⁰.

Comparison with Clever solubilities

The Clever solubilities¹¹⁻¹³ are the only solubility functions that included ample solubility data for temperatures exceeding 50 °C. This high-temperature data was taken exclusively from Morrison and Johnstone (1954)¹⁴, but in the fitting procedure used to generate the Clever solubilities, all of the low-temperature measurements from Morrison and Johnstone (1954) were discarded¹¹⁻¹³, showing that Clever et al. did not give the data too much confidence. The experiments conducted by Morrison and Johnstone (1954) also utilized pure noble gases instead of atmospheric air. For all except krypton and in the high temperature range the Clever solubilities lie far below the newly determined functions (up to -6%). Given this large Clever solubility deviation for high temperatures it is clear that new high temperature measurements were indeed overdue.

Comparison with Weiss solubilities

The Weiss solubilities¹⁹⁻²¹ were determined for He, Ne, Ar and Kr from (0 to 40) °C by completely degassing distilled water and subsequently equilibrating it with pure noble gases. Except for Kr, all Weiss solubility functions lie well below those from this work, with the greatest residuals of $\sim (-0.25 \text{ to } -0.3)\%$ found for He and Ne at 40 °C.

Comparison with Benson-Krause solubilities

The Benson-Krause solubilities²² were determined for He, Ne, Ar, Kr and Xe from (0 to 60) °C with a method similar to that of the Weiss solubilities. They lie neither systematically above nor below those from this work. For Ar and Xe the residuals are fairly low, but

for He, Ne and Kr the residuals exceed $\pm 3\%$.

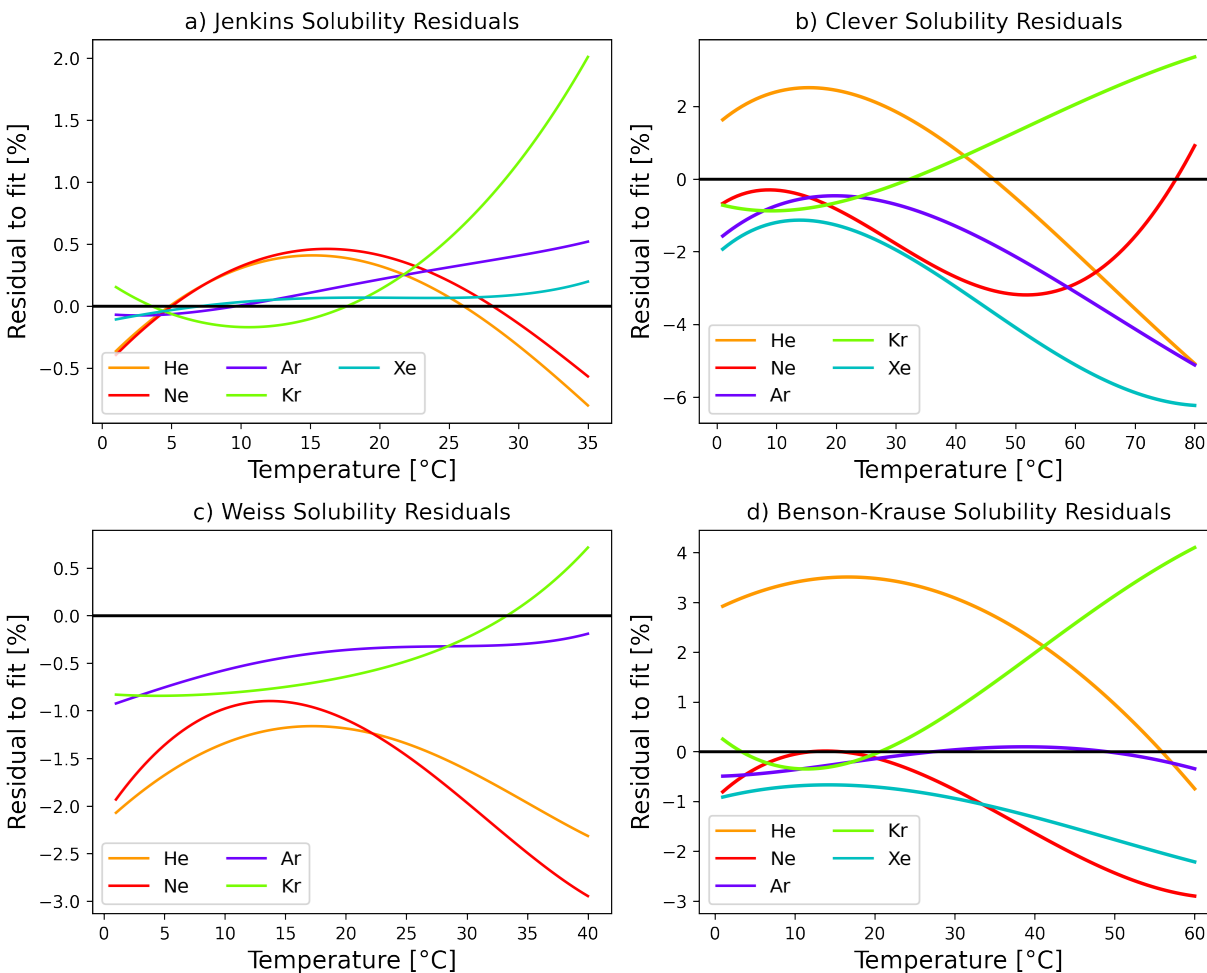


Figure 5: Residuals of the Jenkins¹⁰ (a), Clever¹¹⁻¹³ (b), Weiss¹⁹⁻²¹ (c) and Benson-Krause²² (d) solubility functions to those determined in this work over their respective temperature ranges of validity.

Conclusion and Outlook

With our new data we provide accurate functions for the solubilities of noble gases valid in the temperature range from (0 to 80) °C and for ambient atmospheric pressures. Experiments have been conducted at environmental concentrations of noble gases in the air. The data is consistent with earlier measurements and agrees in general with the expected accuracy. The new measurements clearly document the behaviour against temperature, especially the

continuously decreasing solubility of xenon, krypton and argon versus the less pronounced variability of neon and increasing solubilities of helium towards higher temperatures.

We provide new solubility functions, which, given the standard deviation of residuals seen in Figure 4, can safely be assumed to have relative expanded uncertainties $U_r(L)$ with a 0.99 level of confidence of 0.015 for He and Ar, 0.025 for Xe and 0.030 for Ne and Kr. These solubility functions provide a closed description of solubility over the entire temperature range and hence can be implemented for noble gas thermometry, where a formation of groundwater at higher temperatures cannot be excluded a priori. Especially in volcanic regions on Earth, an equilibration at higher temperatures may occur, as it could be suspected in the case of Lake Kivu³⁶.

Finally, we follow Jenkins et al. (2019)¹⁰ in cautioning the reader not to utilize the solubilities determined in this work to derive absolute Bunsen solubilities or Henry's Law coefficients since the uncertainties in atmospheric abundances must be resolved beforehand. The primary intent of this work is to present noble gas solubility functions that accurately reproduce the abundance of noble gases when an open body of water equilibrates with atmospheric air.

Associated Content

Supporting Information available

In the supporting information we provide an example for typical measurements undertaken during equilibration. We also give a brief overview of some practical unit conversions and necessary physical properties so that readers may easily compare our solubilities with other publications or measurements. Finally, we present for each noble gas separately a more detailed overview of the obtained solubility functions, the utilized data and the residuals of that data to the solubility functions.

References

- (1) Aeschbach-Hertig, W., and Solomon, D. K. In *The noble gases as geochemical tracers*, Burnard, P., Ed.; Advances in Isotope Geochemistry; Springer: 2013, pp 81–122.
- (2) Mazor, E. (1972). Paleotemperatures and other hydrological parameters deduced from gases dissolved in groundwaters, Jordan Rift Valley, Israel. *Geochim. Cosmochim. Acta* 36, 1321–1336.
- (3) Benson, B. (1973). Noble gas concentration ratios as paleotemperature indicators. *Geochim. Cosmochim. Acta* 37, 1391–1395.
- (4) Stute, M., Forster, M., Frischkorn, H., Serejo, A., Clark, J. F., Schlosser, P., Broecker, W. S., and Bonani, G. (1995). Cooling of Tropical Brazil (5°C) during the Last Glacial Maximum. *Science* 269, 379–383.
- (5) Beyerle, U., Purtschert, R., Aeschbach-Hertig, W., Imboden, D., Loosli, H., Wieler, R., and Kipfer, R. (1998). Climate and groundwater recharge during the last glaciation in an ice-covered region. *Science (New York, N.Y.)* 282, 731–734.

- (6) Weyhenmeyer, C., Burns, S., Waber, H., Aeschbach-Hertig, W., Kipfer, R., Loosli, H., and Matter, A. (2000). Cool glacial temperatures and changes in moisture source recorded in oman groundwaters. *Science (New York, N.Y.)* 287, 842–845.
- (7) Stute, M., and Schlosser, P. In *Climate Change in Continental Isotopic Records*, Swart, P. K., Lohmann, K. C., Mckenzie, J., and Savin, S., Eds.; Geophysical Monograph Series; American Geophysical Union: Washington, D. C., 1993, pp 89–100.
- (8) Seltzer, A. M., Ng, J., Aeschbach, W., Kipfer, R., Kulongoski, J. T., Severinghaus, J. P., and Stute, M. (2021). Widespread six degrees Celsius cooling on land during the Last Glacial Maximum. *Nature* 593, 228–232.
- (9) Loose, B., Jenkins, W. J., Moriarty, R., Brown, P., Jullion, L., Naveira Garabato, A. C., Torres Valdes, S., Hoppema, M., Ballentine, C., and Meredith, M. P. (2016). Estimating the recharge properties of the deep ocean using noble gases and helium isotopes. *Journal of Geophysical Research: Oceans* 121, 5959–5979.
- (10) Jenkins, W. J., Lott, D. E., and Cahill, K. L. (2019). A determination of atmospheric helium, neon, argon, krypton, and xenon solubility concentrations in water and seawater. *Marine Chemistry* 211, 94–107.
- (11) *Helium and neon - gas solubilities*; Clever, H. L., Ed.; Solubility data series, Vol. 1; Pergamon Press: Oxford, 1979.
- (12) *Krypton, xenon and radon - gas solubilities*; Clever, H. L., Ed.; Solubility data series, Vol. 2; Pergamon Press: Oxford, 1979.
- (13) Clever, H. L., *Argon*; Solubility data series, Vol. 4; Pergamon Press: Oxford, 1980.
- (14) Morrison, T. J., and Johnstone, N. B. (1954). Solubilities of the inert gases in water. *Journal of the Chemical Society (Resumed)*, 3441.
- (15) Crovetto, R., Fernández-Prini, R., and Japas, M. L. (1982). Solubilities of inert gases and methane in H₂O and in D₂O in the temperature range of 300 to 600 K. *J. Chem. Phys.* 76, 1077–1086.

- (16) Potter, R. W., and Clyne, M. A. (1978). The solubility of the noble gases He, Ne, Ar, Kr, and Xe in water up to the critical point. *Journal of Solution Chemistry* 7, 837–844.
- (17) Smith, S. P., and Kennedy, B. M. (1983). The solubility of noble gases in water and in NaCl brine. *Geochim. Cosmochim. Acta* 47, 503–515.
- (18) Benson, B. B., and Krause, D. (1976). Empirical laws for dilute aqueous solutions of nonpolar gases. *J. Chem. Phys.* 64, 689–709.
- (19) Weiss, R. F. (1970). The solubility of nitrogen, oxygen and argon in water and seawater. *Deep Sea Research and Oceanographic Abstracts* 17, 721–735.
- (20) Weiss, R. F. (1971). Solubility of helium and neon in water and seawater. *J. Chem. Eng. Data* 16, 235–241.
- (21) Weiss, R. F., and Kyser, T. K. (1978). Solubility of krypton in water and seawater. *J. Chem. Eng. Data* 23, 69–72.
- (22) Krause Jr., D., and Benson, B. B. (1989). The solubility and isotopic fractionation of gases in dilute aqueous solution. IIa. solubilities of the noble gases. *J. Solution Chem.* 18, 823–873.
- (23) Boehrer, B., Jordan, S., Leng, P., Waldemer, C., Schwenk, C., Hupfer, M., and Schultze, M. (2021). Gas Pressure Dynamics in Small and Mid-Size Lakes. *Water* 13, 1824.
- (24) Krall, K., and Jähne, B. In *7th SOPRAN Annual Meeting, Bremen, Germany, 25-26 March 2014*, 2014.
- (25) Jähne, B., Heinz, G., and Dietrich, W. (1987). Measurement of the diffusion coefficients of sparingly soluble gases in water. *J. Geophys. Res. C: Oceans* 92, 10767–10776.

- (26) Alduchov, O. A., and Eskridge, R. E. (1996). Improved Magnus Form Approximation of Saturation Vapor Pressure. *Journal of Applied Meteorology* 35, 601–609.
- (27) Wagner, W., and Pruss, A. (1993). International Equations for the Saturation Properties of Ordinary Water Substance. Revised According to the International Temperature Scale of 1990. Addendum to J. Phys. Chem. Ref. Data 16 , 893 (1987). *Journal of Physical and Chemical Reference Data* 22, 783–787.
- (28) IAPWS (1992). Revised Supplementary Release on Saturation Properties of Ordinary Water Substance.
- (29) Beyerle, U., Aeschbach–Hertig, W., Imboden, D. M., Baur, H., Graf, A., and Kipfer, R. (2000). A Mass Spectrometric System for the Analysis of Noble Gases and Tritium from Water Samples. *Environmental Science & Technology* 34, 2042–2050.
- (30) Friedrich, R. Grundwassercharakterisierung mit Umwelttracern: Erkundung des Grundwassers der Odenwald-Region sowie Implementierung eines neuen Edelgas-Massenspektrometersystems. PhD dissertation, Heidelberg: Heidelberg, Ruprecht-Karls-Universität, 2007.
- (31) Kaudse, T. Noble Gases in groundwater of the Azraq Oasis, Jordan and along the central Dead Sea Transform - Two case studies, PhD dissertation, Heidelberg: Heidelberg, Ruprecht-Karls-Universität, 2014.
- (32) Mayer, S. Dynamics of reactive and inert gases in soil air and groundwater in the context of noble gases as environmental tracers, PhD dissertation, Heidelberg: Heidelberg, Ruprecht-Karls-Universität, 2017.
- (33) Virtanen, P., Gommers, R., Oliphant, T. E., Haberland, M., Reddy, T., Cournapeau, D., Burovski, E., Peterson, P., Weckesser, W., Bright, J., van der Walt, S. J., Brett, M., Wilson, J., Millman, K. J., Mayorov, N., Nelson, A. R. J., Jones, E., Kern, R., Larson, E., Carey, C. J., Polat, İ., Feng, Y., Moore, E. W., VanderPlas, J., Laxalde, D., Perktold, J., Cimrman, R., Henriksen, I., Quintero, E. A., Harris, C. R., Archibald, A. M., Ribeiro, A. H., Pedregosa, F., van Mulbregt, P., and SciPy 1.0

- Contributors (2020). SciPy 1.0: Fundamental Algorithms for Scientific Computing in Python. *Nature Methods* 17, 261–272.
- (34) Valentiner, S. (1927). Über die Löslichkeit der Edelgase in Wasser. *Zeitschrift für Physik* 42, 253–264.
- (35) Clarke, E. C. W., and Glew, D. N. (1966). Evaluation of thermodynamic functions from equilibrium constants. *Transactions of the Faraday Society* 62, 539.
- (36) Schwenk, C., Negele, S., Aeschbach, W., and Boehrer, B. (2022). High Temperature Noble Gas Thermometry in Lake Kivu. *In review*.

TOC Graphic

